Inorganic Chemistry

ARTICLE

pubs.acs.org/IC

On the Solvation of the Zn^{2+} Ion in Methanol: A Combined Quantum Mechanics, Molecular Dynamics, and EXAFS Approach

Valentina Migliorati,*[,†] Giovanni Chillemi,[‡] and Paola D'Angelo[†]

[†]Dipartimento di Chimica, Università di Roma "La Sapienza", P.le A. Moro 5, 00185 Roma, Italy

[‡]CASPUR, Inter-University Consortium for Supercomputing in Research, via dei Tizii 6b, 00185 Roma, Italy

ABSTRACT: The solvation properties of the Zn^{2+} ion in methanol solution have been investigated using a combined approach based on molecular dynamics (MD) simulations and extended X-ray absorption fine structure (EXAFS) experimental results. The quantum mechanical potential energy surface for the interaction of the Zn^{2+} ion with a methanol molecule has been calculated taking into account the effect of bulk solvent by the polarizable continuum model (PCM). The effective Zn−methanol interactions have been fitted by suitable analytical potentials, and have been utilized in the MD simulation to obtain the structural properties of the solution. The reliability of the whole procedure has been assessed by comparing the theoretical structural results with the EXAFS experimental data. The structural parameters of the first solvation shells issuing from the MD simulations provide an effective complement to the EXAFS experiments.

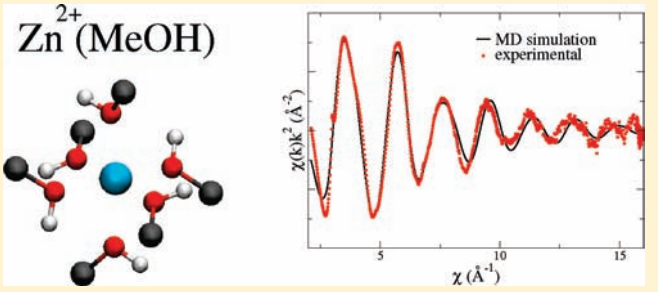

1. INTRODUCTION

Metal ion solvation is one of the most studied areas in solution chemistry, because of its relevance in a large number of physicochemical processes in nature, industrial technology, and living organisms. Water has been by far the most studied solvent,[1] due to its peculiar properties and its ubiquitous character in biological systems. Among the organic solvents, methanol shows intriguing characteristics as it is the simplest organic compound having both a hydrophobic and hydrophilic group. Moreover, methanol is a close analogue to water, because of the presence of the hydroxyl group, and it is able to form a strong network of hydrogen bonds, which is responsible for many properties of the bulk liquid.

A detailed description of the solvent structure and dynamics around a metal ion in solution can be obtained from molecular dynamics (MD) simulations. However, classical MD simulations require analytical potentials to describe the interactions among the atoms, and the use of proper interaction potentials is crucial to obtain reliable results. As concerns the methanol−methanol interactions, several models are available in the literature which were developed to reproduce experimental properties of pure methanol.[2−5] As far as the ion−solvent interactions are concerned, two different strategies are present in the literature. The former relies on the use of empirical potentials optimized to reproduce suitable experimental data. In this context, Ca^{2+}−methanol interaction potentials have been developed to reproduce the experimental solvation enthalpy and hydration number of a diluted Ca^{2+} methanol solution.[6] In the case of alkali ions, empirical interaction potentials optimized for water[7] were subsequently used in MD simulations of methanol solutions.[8] This approximation was shown to be reasonable as it produced a theoretical determination of the solvation free energies of cations in methanol in good agreement with the experimental data.[8] A major drawback of empirical potentials is that even if they properly reproduce the experimental properties for which they were developed, they are often not able to provide a correct determination of other structural, energetic, and dynamic properties of the system.

The latter approach is to parametrize the ion−solvent interaction potential using quantum mechanical (QM) methods. This strategy has been adopted to generate Mg^{2+}−methanol,[9] Ca^{2+}−methanol[10,11] and Na^{+}−methanol[12] pair potentials, by carrying out ab initio calculations on a system composed by the ion and one methanol molecule in vacuum. Such calculations completely neglect the so-called many body effects,[13] which have to be taken into account to properly describe the ion−solvent interactions, especially when dealing with multiply charged cations.[13] In the case of cation−methanol interactions the polarization of solvent molecules in the electric field of the cation and the charge transfer from methanol to the cation are the main sources of many body interactions. Both these effects give rise to binding interactions that are reduced in the presence of several solvent molecules. An efficient way to include many body effects in the ion−solvent potential is to consider the solvent contribution in an implicit way by means of the polarizable continuum model (PCM).[14] The PCM method has been successfully used to develop effective potentials for several cations in water.[15−18] These potentials were then employed in classical MD simulations, and the

Received: May 24, 2011
Published: July 29, 2011

reliability of the computational procedure was assessed by comparing the theoretical structural results with the X-ray absorption spectroscopy (XAS) experimental data.[19−23]

Here, we have undertaken an experimental and theoretical investigation of the Zn^{2+} ion in methanol solution. In particular, we used a combination of QM calculations, classical MD simulations, and extended X-ray absorption fine structure (EXAFS) spectroscopy, and this joint approach allowed us to obtain very accurate structural information on the Zn^{2+} solvation complex in methanol.

2. METHODS

2.1. Computational Procedure. The computational procedure consists of three steps: (i) generation of the ab initio potential energy surface (PES) of the Zn^{2+}−methanol system with the inclusion of the averaged many body effects by means of the so-called conductor-like PCM (CPCM); (ii) fitting of the PES with a suitable functional form of the ion−methanol interaction potential; (iii) inclusion of the effective two-body potential in the GROMACS MD code[24] and system simulation.

2.1.1. Generation of the Ion−Methanol ab Initio PES. In the first step of our procedure an effective Zn^{2+}−methanol pair potential function (U_{ZnMet}) is calculated along the line of the method proposed by Floris et al.[25] and previously applied to the study of several cations in water.[15−18] The average many-body effects are accounted for by using the following expression

$$U_{ZnMet} = \langle\Psi|\hat{H}^{(0)}|\Psi\rangle_{ZnMet} - \langle\Psi|\hat{H}^{(0)}|\Psi\rangle_{Zn} - \langle\Psi|\hat{H}^{(0)}|\Psi\rangle_{Met} \quad (1)$$

where the wave function Ψ is perturbed by the solvent effects according to the CPCM, while the Hamiltonian operators are those of Zn^{2+}−methanol, bare Zn^{2+} ion, and bare methanol molecule in vacuum. In this definition of U_{ZnMet} the interaction energies with the dielectric continuum have been removed because during the MD simulation the continuum is replaced by explicit solvent molecules which interact with the cation and the other methanol molecules according to their respective interaction potentials.

The difference between the wave function calculated in vacuum and with the PCM depends on the dielectric constant of the solvent (32.63 for methanol), and on the shape of the cavity in which the Zn^{2+}−methanol system is embedded. The cavity is modeled as a set of interlocking spheres centered on the atomic nuclei and for neutral species the sphere radius (R_s) is generally set to $R_s = 1.2\ R_{vdW}$ where R_{vdW} is the van der Waals radius of the atom.[25] We have thus employed R_s = 1.68 and 1.44 Å for oxygen and hydrogen, respectively. Following the Pauling's formulation of the van der Waals radii,[26] the methyl group of the methanol molecule has been treated as a united atom, with a single sphere centered on the carbon atom with R_s = 2.4 Å. The choice of the radius for the ion cavity is somehow more arbitrary, and we have decided to retain the Zn^{2+} cavity radius (R_s = 0.904 Å) previously optimized for water.[16] However, we have checked that the internal consistency criterium used for the optimization of the cation cavity radius in water was verified also in the present case. According to this criterium if the perturbation induced by the ion is of the right magnitude, we should have

$$U_{MetZnMet} = 2U_{ZnMet} + U_{MetMet} \quad (2)$$

where U_{MetMet} is the methanol−methanol potential while $U_{MetZnMet}$ is the interaction energy of a cluster composed by one Zn^{2+} ion and two solvent molecules (MetZnMet), given by

$$U_{MetZnMet} = \langle\Psi|\mathbf{H}^{(0)}|\Psi\rangle_{MetZnMet} - 2\langle\Psi|\mathbf{H}^{(0)}|\Psi\rangle_{Met} - \langle\Psi|\mathbf{H}^{(0)}|\Psi\rangle_{Zn} \quad (3)$$

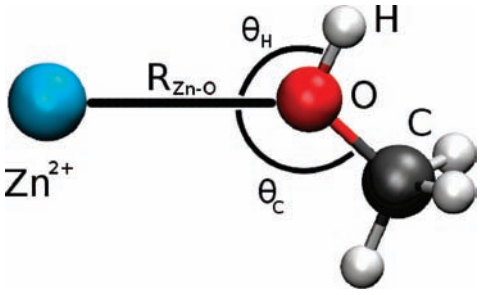

Figure 1. Definition of the Zn^{2+}−methanol geometrical parameters used for the generation of the ab initio potential energy surface.

The interaction energies have been computed for a Zn−O distance of 2.2 Å and a MetZnMet complex with a face-to-face C_2 symmetry of the two ligands and an O−Zn−O angle of 90°, as suggested by Floris et al.[25] By using the Zn^{2+} cavity radius optimized for water, we have calculated the left and right sides of eq 2 (−769 240 and −769 245 kJ mol^{-1}, respectively), and we have found that their difference is very low. The error associated with the use of the cavity radius adopted for water can thus be considered acceptable for the classical model of interactions we utilize in this work. Each sphere forming the solute cavity has been subdivided into finite elements (tesserae) with constant average area of 0.2 $Å^2$ without any charge compensation.[27]

All of the QM calculations have been carried out with the Gaussian98 package,[28] using the Hartree−Fock method, with the LANL2DZ effective core potential and valence basis set[29−31] for the Zn^{2+} ion and the cc-pVTZ basis set[32] for the methanol molecule. Note that first row transition metals can be successfully studied also by using all electron basis sets.[33,34] Our choice to use LANL2DZ is motivated by the fact that there is a substantial saving of computer time when using the LANL2DZ pseudopotential and valence basis set as compared to all electron basis sets of comparable quality. However, some trial tests have shown that the interaction energies change less than 2% when all electron basis sets are used in the calculations.

In order to verify if this basis set is able to reproduce the partial charges of the OPLS methanol model which will be employed in the MD simulation, we have carried out a QM energy calculation and charge fitting of the molecular electrostatic potential by the CHelpG procedure,[35] using the PCM and the same computational set up employed for the PES calculations. The methanol geometry chosen is the experimental one with the hydrogen atoms of the methyl group in the staggered equilibrium positions.[36] The OPLS model is a rigid three site model with partial charges of −0.700, 0.435, and 0.265 a.u. on the oxygen, hydrogen atom, and methyl group, respectively.[3,4] By treating the CH_3 group as a united atom, we have obtained partial charges of −0.740, 0.440, and 0.300 a.u. that are in good agreement with the OPLS ones.

The PES of the Zn^{2+}−methanol system has been characterized by means of 2397 grid points. The methanol molecule was kept fixed at the experimental geometry during the PES calculation. As sketched in Figure 1, we adopted an internal coordinate system, and we carried out several energy scan jobs along the ion−oxygen distance (R_{Zn-O}), varying either the θ_H or the θ_C angle. In particular, the ion−oxygen distance was varied in the range $1.2 \le R_{Zn-O} \le 4.0$ Å and a step of 0.02 Å, with θ_H ranging from 25° to 125°, and θ_C ranging from 65° to 115° with a step of 10°, while keeping Zn^{2+} on the plane spanned by O, H, and C. Note that since methanol is kept rigid during the PES scans, the θ_H and θ_C angles are associated with the same degree of freedom and for this reason they have not been varied simultaneously in the PES calculations. It is important to stress that the ab initio energies have been computed for ion−oxygen distances only up to 4 Å, since after this distance value the ion−methanol interaction is essentially Coulombic

dx.doi.org/10.1021/ic201100q |Inorg. Chem. 2011, 50, 8509–8515

Table 1. Estimated Zn^{2+}−Methanol Interaction Parameters and Relative Standard Deviations

	param	std dev
A_o (kJ mol^{-1} nm^4)	-3.494×10^{-1}	4.06×10^{-3}
B_o (kJ mol^{-1} nm^6)	2.470×10^{-3}	4.07×10^{-5}
C_o (kJ mol^{-1} nm^8)	-2.420×10^{-6}	5.90×10^{-8}
D_o (kJ mol^{-1} nm^{12})	-8.080×10^{-10}	2.85×10^{-12}
E_o (kJ mol^{-1})	$3.899 \times 10^{+5}$	$9.35 \times 10^{+3}$
F_o (nm^{-1})	$4.148 \times 10^{+1}$	1.95×10^{-1}
A_h (kJ mol^{-1} nm^4)	6.870×10^{-2}	3.36×10^{-4}
B_h (kJ mol^{-1} nm^6)	-4.700×10^{-4}	7.40×10^{-6}
C_h (kJ mol^{-1} nm^8)	2.462×10^{-6}	4.63×10^{-8}
D_h (kJ mol^{-1} nm^{12})	-2.430×10^{-11}	4.85×10^{-13}
A_c (kJ mol^{-1} nm^4)	1.475	0.43×10^{-2}
B_c (kJ mol^{-1} nm^6)	-7.990×10^{-2}	3.38×10^{-4}
C_c (kJ mol^{-1} nm^8)	1.650×10^{-3}	7.70×10^{-5}
D_c (kJ mol^{-1} nm^{12})	-2.100×10^{-7}	1.11×10^{-9}

and this contribution to the interaction energy is known "a priori" from the partial charges of the ion and of the solvent model.

The initial 2397 grid points were reduced to 2379 by imposing a threshold of 2500 kJ mol^{-1} for the interaction energy, thus not including the most repulsive conformations in the PES. This procedure of energy filtering allows one to significantly improve the quality of the fitting results.

2.1.2. Fitting Procedure. The Zn^{2+}−methanol ab initio interaction energies have been fitted using the following analytical function

$$V(r) = \frac{q_i q_o}{r_{io}} + \frac{A_o}{r_{io}^4} + \frac{B_o}{r_{io}^6} + \frac{C_o}{r_{io}^8} + \frac{D_o}{r_{io}^{12}} + E_o e^{-F_o r_{io}} + \frac{q_i q_h}{r_{ih}} + \frac{A_h}{r_{ih}^4} + \frac{B_h}{r_{ih}^6} + \frac{C_h}{r_{ih}^8} + \frac{D_h}{r_{ih}^{12}} + \frac{q_i q_c}{r_{ic}} + \frac{A_c}{r_{ic}^4} + \frac{B_c}{r_{ic}^6} + \frac{C_c}{r_{ic}^8} + \frac{D_c}{r_{ic}^{12}} \quad (4)$$

where r_{io}, r_{ih}, and r_{ic} are the ion−methanol distances and q_i, q_o, q_h, and q_c are the electrostatic charges of the cation (2 a.u.), the oxygen and hydrogen atoms, and the methyl group in the OPLS methanol model, respectively. A_o,..., F_o; A_h,..., D_h; and A_c,..., D_c are the unknown parameters. The fitting was carried out by means of the Newton method as implemented in the statistic package SAS, which is a commercial statistical analysis system, designed for fast statistical computation. SAS consists primarily of built-in subroutines but via the interactive matrix language allows also users to program their own procedures and run them with it.[37] All of the resulting Zn^{2+}−methanol parameters are listed in Table 1, together with their standard deviations. The differences between the energies calculated with the effective two-body potential of eq 4 and the original ab initio values have a standard deviation of 17 kJ mol^{-1}, in agreement with previous results.[16,17] The fitted Zn^{2+}−methanol energy curve is compared in Figure 2 with the effective Zn^{2+}−water interaction potential previously derived using the same computational setup.[16] Note that both functions refer to an antidipole orientation of the solvent molecule with respect to the ion. As it can be seen, the two curves show a very similar trend. The minimum energy values differ of only 5% of the well depth (−258 and −245 kJ mol^{-1} for methanol and water, respectively), and the corresponding Zn−O distances are very close (1.93 and 1.95 Å for methanol and water, respectively).

2.1.3. MD Simulation and Structural Analysis. The newly developed Zn^{2+}−methanol potential has been included in the GROMACS package[24] while the OPLS model has been used for the methanol−methanol interactions, as it correctly describes many properties of liquid methanol.[38] Moreover, in a combined MD-EXAFS investigation of Sr^{2+} in methanol solution, the performances of several methanol models were compared and the OPLS model was found to provide the best agreement with the EXAFS experimental data.[39] The MD simulation was carried out on a system composed by one Zn^{2+} ion and 819 methanol molecules in a cubic box of 38.1 Å edge length, using periodic boundary conditions.

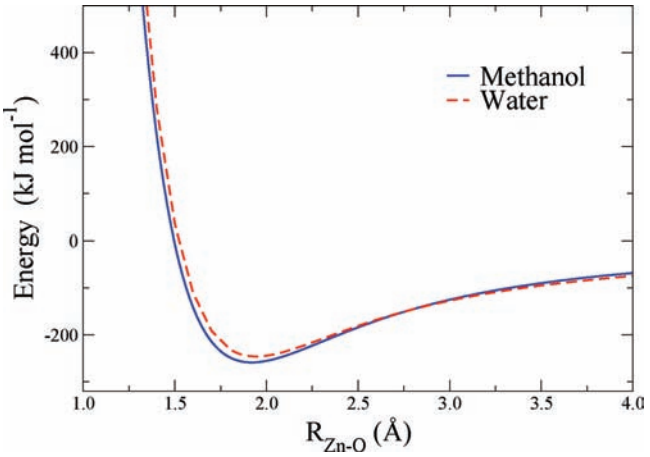

Figure 2. Comparison between the fitted Zn^{2+}−methanol interaction potential and the Zn^{2+}−water interaction potential previouly obtained in ref 16 as a function of the Zn−O distance (R_{Zn-O}). Both functions refer to an antidipole orientation of the solvent molecule with respect to the ion.

In order to compare the structural properties of the Zn^{2+} solvation complex in methanol and aqueous solution, we carried out also an MD simulation of Zn^{2+} in water. The system was composed of one Zn^{2+} ion and 819 water molecules in a cubic box of 29.0 Å box length with periodic boundary conditions. The simulation has been performed using an effective Zn−water two-body potential obtained by fitting the parameters of a suitable analytical function on an ab initio PES, as thoroughly described in ref 16. As far as the water−water interactions are concerned, the SPC/E water model was used which provides a very good description of the structural and dynamic properties of liquid water.[40]

Both the methanol and aqueous solutions were simulated in an NVT ensemble, where the temperature was kept fixed at 300 K using the Berendsen method[41] with a coupling constant of 0.1 ps. A cutoff of 9 Å has been used for the nonbonded interactions, using the particle mesh Ewald method to calculate the long-range electrostatic interactions.[42] The simulations have been carried out for 13 ns, with a time step of 1 fs. The first 3 ns have been used for equilibration and discarded in the following analyses.

The structural properties of the Zn^{2+} ion in methanol and aqueous solution are described in terms of radial distribution functions, $g_{Zn-O}(r)$, $g_{Zn-H}(r)$, and $g_{Zn-C}(r)$

$$g_{AB}(r) = \frac{\langle \rho_B(r) \rangle}{\langle \rho_B \rangle_{local}} = \frac{1}{N_A \langle \rho_B \rangle_{local}} \sum_{i \in A}^{N_A} \sum_{i \in B}^{N_B} \frac{\delta(r_{ij} - r)}{4\pi r^2} \quad (5)$$

where $\langle \rho_B(r) \rangle$ is the particle density of type B at distance r around type A, and $\langle \rho_B \rangle_{local}$ is the particle density of type B averaged over all spheres around particle A with radius r_{max} (half the box length).

Angular distribution functions have been calculated for three different angles: the angle formed by two Zn−O vectors in the first coordination shell (labeled as ψ), the angle formed by the Zn−O and O−H vectors (labeled as ω), and the angle formed by the solvent molecule dipole and the Zn−O vector direction (labeled as ϕ).

dx.doi.org/10.1021/ic201100q |*Inorg. Chem.* 2011, 50, 8509–8515

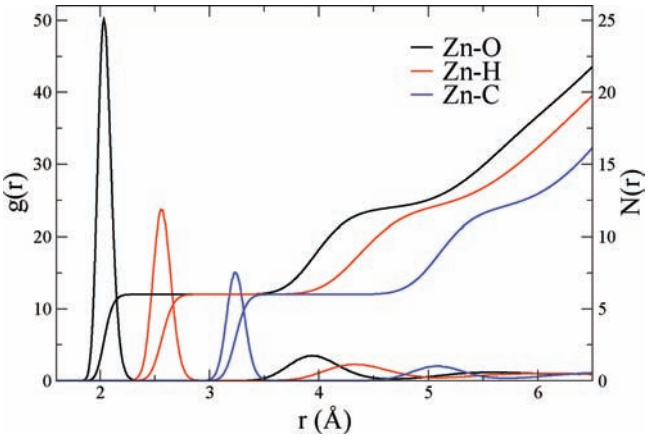

Figure 3. Zn−O (black line), Zn−H (red line), and Zn−C (blue line) radial distribution functions calculated from the MD simulation. Running integration numbers are also shown.

2.2. X-ray Absorption Measurements and EXAFS Data Analysis. A 0.1 M Zn^{2+} methanol solution was prepared by dissolving the appropriate amount of $Zn(CF_3SO_3)_2$ in methanol. Zn K-edge X-ray absorption spectra were obtained using the EMBL spectrometer at DESY.[43] Spectra were recorded in transmission mode using a Si(211) double-crystal monochromator detuned to 30% for harmonic rejection.[44] Data points were collected for 1 s each, and three spectra were recorded and averaged after performing an absolute energy calibration.[44] The DORIS III storage ring was running at an energy of 4.4 GeV with positron currents between 120 and 90 mA. The solution was kept in a cell with Kapton film windows and a Teflon spacer of 2 mm.

In conventional EXAFS data analysis of disordered systems the $\chi(k)$ signal is represented by the equation

$$\chi(k) = \int_0^\infty dr\, 4\pi r^2 \rho(r) A(k,r) \sin[2kr + \phi(k,r)] \qquad (6)$$

where $A(k,r)$ and $\phi(k,r)$ are the amplitude and phase functions, respectively, and ρ is the density of the scattering atoms. $\chi(k)$ theoretical signals can be calculated by introducing in eq 6 the model radial distribution functions obtained from MD simulations. The EXAFS theoretical signals have been calculated by means of the GNXAS program, and a thorough description of the theoretical framework can be found in ref 45. Phase shifts, $A(k,r)$ and $\phi(k,r)$, have been calculated starting from one of the MD configurations, by using muffin-tin potentials and advanced models for the exchange-correlation self-energy (Hedin−Lundqvist). The values of the muffin-tin radii are 0.2, 0.9, 0.7, and 1.2 Å, for hydrogen, oxygen, carbon, and zinc, respectively. Inelastic losses of the photoelectron in the final state have been accounted for intrinsically by complex potential. The imaginary part also includes a constant factor accounting for the core-hole width (1.67 eV). The Zn−O, Zn−H, and Zn−C $g(r)$ values obtained from the methanol MD simulation have been used to calculate the single scattering first shell $\chi(k)$ theoretical signal, as the ion-hydrogen interactions have been found to provide a detectable contribution to the EXAFS spectra of several metal ions in aqueous solutions,[20,46,47] and no optimization of the structural parameters has been carried out. As far as the nonstructural parameters are concerned, the energy difference between the experimental and theoretical scale (E_0) and the amplitude correction factor S_0^2 have been kept fixed to the values determined from the EXAFS analysis of Zn^{2+} in water (E_0 = 1.6 eV and S_0^2 = 0.99).[46] The background function used to extract the $\chi(k)$ experimental signal has been modeled by means of step-shaped functions to account for the 1s3p and 1s3s double-electron resonances. The energy onsets and the intensities of these channels are those reported in Table 2 of ref 46.

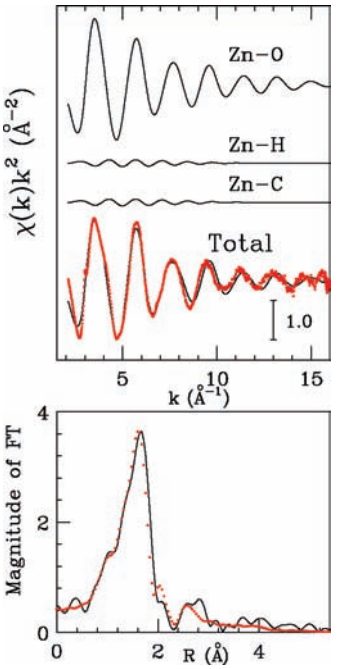

Figure 4. Upper panel: Comparison between the EXAFS experimental data (dotted red line) and the theoretical signal calculated from the Zn−O, Zn−H, and Zn−C $g(r)$'s obtained from the MD simulation of Zn^{2+} in methanol solution (solid black line). H refers to the hydrogen atom bonded to the oxygen atom of the methanol molecule. Lower panel: Non-phase-shifted corrected Fourier transforms of the EXAFS experimental data (dotted red line) and of the theoretical signal (solid black line).

3. RESULTS AND DISCUSSION

The Zn−O, Zn−H, and Zn−C radial distribution functions ($g(r)$'s) and the corresponding running integration numbers calculated from the methanol MD simulation are shown in Figure 3. The $g(r)$'s show very sharp and separated first peaks followed by depletion zones, indicating the existence of a stable first solvation shell and of a preferential orientation of solvent molecules in the first coordination sphere. The three $g(r)$'s are almost Gaussian in shape, and the maximum of the distribution coincides with the modal value. The first maximum positions of the Zn−O, Zn−H, and Zn−C $g(r)$'s are found at 2.04, 2.56, and 3.24 Å, respectively. The first shell coordination number obtained by integration of the Zn−O $g(r)$ up to the first minimum is 6, and no solvent exchange events have been observed between the first and second coordination sphere during the entire simulation time.

A first check of the reliability of the computational procedure used in this work can be performed by comparing the structural results obtained from our MD simulation with the EXAFS experimental results of ref 48. The Zn−O first shell distance and coordination number are 2.08 Å and 6, respectively, as determined by the EXAFS analysis carried out assuming Gaussian atomic distributions,[48] and a close agreement between our theoretical results and experiment is found for both structural parameters.

dx.doi.org/10.1021/ic201100q |Inorg. Chem. 2011, 50, 8509–8515

Direct comparison of the MD structural results with the EXAFS experimental data allows the accuracy of the simulation to be definitely proved. $\chi(k)$ theoretical signals have been calculated by means of eq 6 starting from the Zn−O, Zn−H, and Zn−C $g(r)$'s. The structural parameters derived from the simulations were kept fixed during the EXAFS analysis. In this way the first coordination shell structure obtained from the simulation can be directly compared with the experimental data.

In the upper panel of Figure 4, we show the comparison between the experimental EXAFS spectrum of Zn^{2+} in methanol and the theoretical curves obtained from the MD simulations. The first three curves from the top are the Zn−O, Zn−H, and Zn−C first shell contributions calculated from the MD $g(r)$'s without any adjustable parameter, while the reminder of the figure shows the total theoretical signal compared with the experimental spectrum. Note that even if the Zn−O two body signal provides the most important contribution to the total $\chi(k)$ function, the hydrogen atoms in the first hydration shell give rise to a sizable contribution in the k region up to 9 $Å^{-1}$. The importance of the hydrogen contribution to the EXAFS spectra of metal cations in aqueous solution has been pointed out in several previous works.[20,46,47]

The theoretical $\chi(k)$ signal matches the experimental data very well, showing that the structural information derived from the MD simulation is basically correct. This finding is reinforced by the Fourier transform (FT) moduli of the EXAFS $\chi(k)$ theoretical and experimental signals shown in the lower panels of Figure 4. The FTs have been calculated in the k-range 2.1−15.0 $Å^{-1}$ with no phase shift correction applied.

Once the validity of our computational procedure has been assessed, it is interesting to compare the MD structural results of the methanol solution with those previously obtained for Zn^{2+} in water,[16] due to the similar nature of the ion−methanol and ion−water interactions. In aqueous solution the Zn^{2+} ion is well-known to be strongly coordinated by six water molecules in an octahedral symmetry,[16,46,49] and the residence time of water molecules in the first hydration shell of Zn^{2+} is estimated to be in the microsecond time scale.[50] The present results show that the solvation structure of Zn^{2+} in water and methanol is very similar, as it is characterized by a similar first shell distance (the position of the Zn−O $g(r)$ first peak is 2.07 Å in aqueous solution[46]) and by the same coordination number. A similar structure of the first shell coordination complex in water and methanol was previously found for Na^+ from two theoretical investigations,[12,51] while a recent MD study of a $CaCl_2$ methanol solution inferred that the Ca^{2+} ion coordinates fewer methanol than water molecules.[11]

Note that the Zn−O $g(r)$ first peak is about 2.5 times higher than that obtained in aqueous solution,[16] and similar differences were previously observed for other ions.[10−12] Such a behavior has been partly attributed to the stronger ion−methanol interactions as compared to the ion−water ones,[10,12] but in our opinion this is a very minor effect. By definition, the peaks of a $g(r)$ function represent the structure relative to the bulk, and the higher first peak in the ion−O $g(r)$ of methanol means that there is more structuring relative to bulk in methanol than in water. This is largely due to the lower bulk density of oxygen atoms in methanol as a consequence of the larger molar volume of the methanol molecules as compared to water.

The second solvation shell of the Zn^{2+} ion in methanol is represented by a broad peak of the Zn−O $g(r)$, located between 3.25 and 4.70 Å, with a maximum at 3.94 Å. The number of methanol molecules in the second solvation shell calculated by the integration of the Zn−O $g(r)$ up to the second minimum is 6. The second hydration shell of the Zn^{2+} ion is much more populated and contains about twice as many solvent molecules.[16] This is most probably due to the fact that the replacement of the hydrogen atom of water with the bulky methyl group of methanol allows the formation of only one hydrogen bond per methanol molecule, on average, between the first and second solvation sphere, while in the case of water two hydrogen bonds per water molecule can be expected.

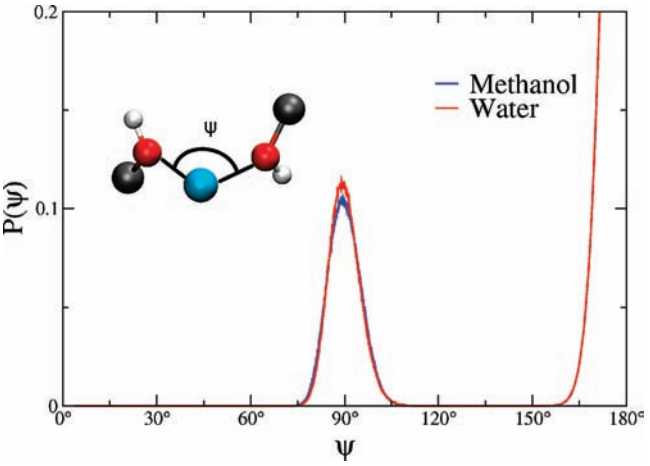

Figure 5. O−Zn−O ψ angular distribution functions obtained from the MD simulations of the Zn^{2+} ion in methanol (blue line) and water (red line).

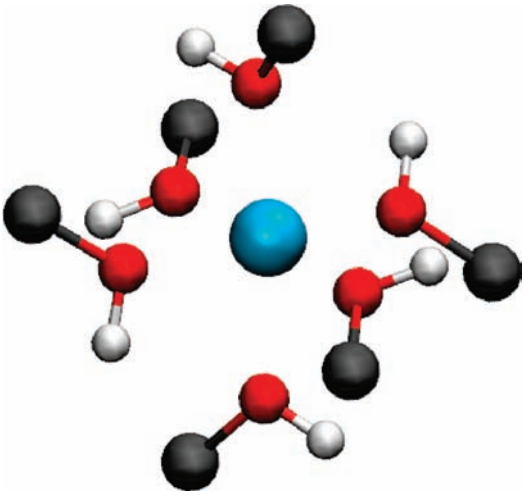

Figure 6. Coordination geometry of the Zn^{2+} ion as obtained from one MD snapshot.

The geometrical arrangement of the first shell methanol molecules around the Zn^{2+} ion can be evaluated by looking at the angular distribution functions of the O−Zn−O ψ angle, plotted in Figure 5 together with the same distribution calculated from the MD simulation of Zn^{2+} in aqueous solution. The two functions are almost identical and have coincident maxima for ψ values of 90° and 180°, thus showing the existence of a stable octahedral geometry in both cases. Moreover, the angular distribution functions go to zero for intermediate values, as solvent molecules are strongly constrained in their positions and large distortions of the octahedral symmetry are expected neither in

dx.doi.org/10.1021/ic201100q |*Inorg. Chem.* 2011, 50, 8509–8515

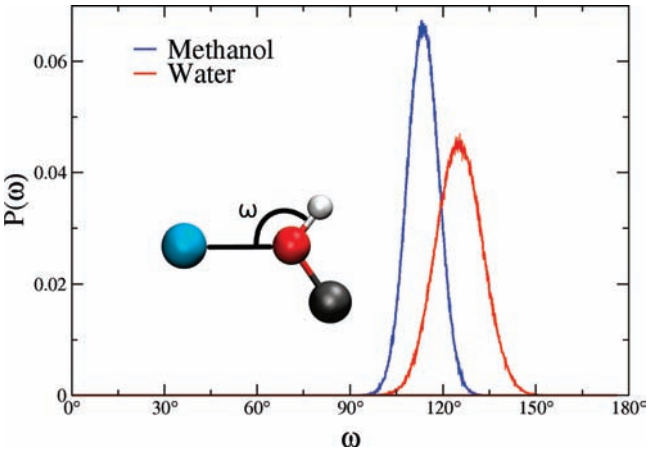

Figure 7. ω angular distribution functions obtained from the MD simulations of the Zn^{2+} ion in methanol (blue line) and water (red line).

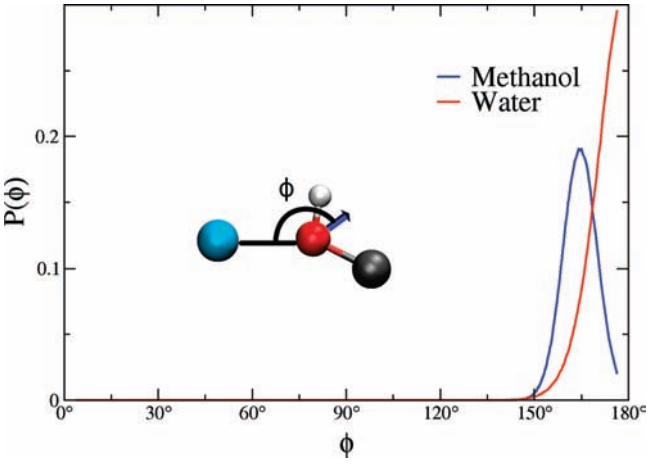

Figure 8. ϕ angular distribution functions obtained from the MD simulations of the Zn^{2+} ion in methanol (blue line) and water (red line).

methanol nor in water. Interestingly, the identity of the angular distribution widths obtained for the two solvents indicates that the relative motional freedom of the first shell oxygen atoms is exactly the same in methanol and water. In Figure 6 a MD snapshot is shown highlighting the coordination geometry of the Zn^{2+} ion.

The orientation of a single methanol molecule in the first solvation shell can be inferred from the distribution of the ω angle, which is compared with the ω distribution obtained for water in Figure 7. In both cases the distributions show well-defined peaks, but the positions of the maxima are different in the two simulations (ω = 113.6° and ω = 125.5° for methanol and water, respectively). The angular function calculated from the MD simulation of the aqueous solution is consistent with an antidipole orientation of the water molecules, while the results of the methanol solution suggest a deviation from this orientation. The ω distribution obtained for water is broader and less intense, indicating a higher flexibility and larger orientational freedom of the water molecules belonging to the Zn^{2+} first coordination sphere as compared to the methanol ones. Altogether the results of the ψ and ω angle analysis suggest that the effect of the increased steric hindrance of methanol is to hamper the rotation of the individual methanol molecules in the first solvation shell. Conversely, the relative mobility of first shell solvent molecules is the same.

A deeper insight into the orientation of the solvent molecules in the first coordination sphere can be gained by calculating the distribution of the ϕ angle (Figure 8). The sharp peak located at 180° obtained for water demonstrates the presence of an antidipole orientation of the water molecules in the Zn^{2+} first hydration sphere. Conversely, a sharp peak with maximum at 164° is found for methanol, which indicates that the dipole moments of the methanol molecules belonging to the Zn^{2+} first coordination shell are tilted by about 16° from the antidipole arrangement. However, the sharpness of the peak in both distributions is due to the strong structuring ability of the Zn^{2+} ion. As concerns the methanol dipole orientation in the proximity of a metal ion, different MD results have been reported in the literature depending on the nature of the cation under investigation. As an example, for Na^{+12} and Sr^{2+39} an antidipole arrangement was found, while in the case of the Ca^{2+} ion a deviation of about 25° from this orientation was inferred.[11]

4. CONCLUSIONS

In the present work we have investigated the coordination properties of the Zn^{2+} ion in methanol using an integrated approach which combines QM calculations, classical MD simulations, and EXAFS experimental data. In particular, an effective two body potential for the Zn^{2+}—methanol interaction has been derived from ab initio calculations taking into account the effect of bulk solvent by the PCM method. This newly developed interaction potential has been used in the MD simulation to derive the structural properties of the solution. The reliability of the whole computational procedure has been assessed by comparing the MD structural results with the EXAFS spectra, and an excellent agreement between theory and experiment has been obtained. Finally, the structural properties of the Zn^{2+} ion in methanol and water have been compared. A very similar octahedral first shell complex has been found in both cases, while the main difference between the two solvents is the smaller orientational freedom of the individual methanol molecules in the Zn^{2+} first coordination sphere as compared to the water ones, as a result of the increased steric hindrance of the methanol molecule.

AUTHOR INFORMATION

Corresponding Author

*E-mail: v.migliorati@caspur.it.

ACKNOWLEDGMENT

This work was supported by CASPUR with the Standard HPC Grant 2011 entitled "A Combined X-ray Absorption Spectroscopy, Molecular Dynamics Simulations and Quantum Mechanics Calculation Procedure for the Structural Characterization of Ill-Defined Systems".

REFERENCES

(1) Ohtaki, H.; Radnai, T. *Chem. Rev.* **1993**, *93*, 1157–1204.
(2) Haughney, M.; Ferrario, M.; McDonald, I. R. *J. Phys. Chem.* **1987**, *91*, 4934–4940.
(3) Jorgensen, W. L. *J. Am. Chem. Soc.* **1981**, *103*, 341–345.
(4) Jorgensen, W. L. *J. Phys. Chem.* **1986**, *90*, 1276–1284.
(5) Stouten, P. F.; Kroon, J. *J. Mol. Struct.* **1988**, *177*, 467–475.

(6) Dang, L. X.; Schenter, G. K.; Fulton, J. L. *J. Phys. Chem. B* **2003**, *107*, 14119–14123.
(7) Aaqvist, J. *J. Phys. Chem.* **1990**, *94*, 8021–8024.
(8) Aaqvist, J.; Alvarez, O.; Eisenman, G. *J. Phys. Chem.* **1992**, *96*, 10019–10025.
(9) Tamura, Y.; Spohr, E.; Heinzinger, K.; Pálinkás, G.; Bakó, I. *Ber. Bunsenges. Phys. Chem.* **1992**, *96*, 147–158.
(10) Kosztolányi, T.; Bakó, I.; Pálinkás, G. *J. Mol. Liq.* **2006**, *126*, 1–8.
(11) Owczarek, E.; Hawlicka, E. *J. Phys. Chem. B* **2006**, *110*, 22712–22718.
(12) Marx, D.; Heinzinger, K.; Pálinkás, G.; Bakó, I. *Z. Naturforsch., A: Phys Sci.* **1991**, *46*, 887–897.
(13) Elrod, M. J.; Saykally, R. J. *Chem. Rev.* **1994**, *94*, 1975–1997.
(14) Amovilli, C.; Barone, V.; Cammi, R.; Cances, E.; Cossi, M.; Mennucci, B.; Pomelli, C. S.; Tomasi, J. *Adv. Quantum Chem.* **1999**, *32*, 227.
(15) Floris, F. M.; Tani, A. *J. Chem. Phys.* **2001**, *115*, 4750–4765.
(16) Chillemi, G.; D'Angelo, P.; Pavel, N. V.; Sanna, N.; Barone, V. *J. Am. Chem. Soc.* **2002**, *124*, 1968–1976.
(17) Chillemi, G.; Barone, V.; D'Angelo, P.; Mancini, G.; Persson, I.; Sanna, N. *J. Phys. Chem. B* **2005**, *109*, 9186–9193.
(18) Chillemi, G.; Mancini, G.; Sanna, N.; Barone, V.; Longa, S. D.; Benfatto, M.; Pavel, N. V.; D'Angelo, P. *J. Am. Chem. Soc.* **2007**, *129*, 5430–5436.
(19) Mancini, G.; Sanna, N.; Barone, V.; Migliorati, V.; D'Angelo, P.; Chillemi, G. *J. Phys. Chem. B* **2008**, *112*, 4694–4702.
(20) D'Angelo, P.; Migliorati, V.; Mancini, G.; Chillemi, G. *J. Phys. Chem. A* **2008**, *112*, 11833–11841.
(21) D'Angelo, P.; Zitolo, A.; Migliorati, V.; Mancini, G.; Persson, I.; Chillemi, G. *Inorg. Chem.* **2009**, *48*, 10239.
(22) D'Angelo, P.; Migliorati, V.; Mancini, G.; Barone, V.; Chillemi, G. *J. Chem. Phys.* **2008**, *128*, 84502.
(23) Migliorati, V.; Mancini, G.; Chillemi, G.; Zitolo, A.; D'Angelo, P. *J. Phys. Chem. A* **2011**, *115*, 4798–4803.
(24) Berendsen, H. J. C.; van der Spoel, D.; van Drunen, R. *Comput. Phys. Commun.* **1995**, *91*, 43–56.
(25) Floris, F.; Persico, M.; Tani, A.; Tomasi, J. *Chem. Phys. Lett.* **1992**, *199*, 518–524.
(26) Pauling, L. *The Nature of the Chemical Bond*, 2nd ed.; Cornell University Press: Ithaca, NY, 1946.
(27) Cossi, M.; Rega, N.; Scalmani, G.; Barone, V. *J. Comput. Chem.* **2003**, *24*, 669–681.
(28) Frisch, J. R.; Trucks, G. W.; Schlegel, H. B.; Scuseria, G. E.; Robb, M. A.; Cheeseman, J. R.; Zakrzewski, V. G.; Montgomery, J. A., Jr.; Stratmann, R. E.; Burant, J. C.; Dapprich, S.; Millam, J. M.; Daniels, A. D.; Kudin, K. N.; Strain, M. C.; Farkas, O.; Tomasi, J.; Barone, V.; Cossi, M.; Cammi, R.; Mennucci, B.; Pomelli, C.; Adamo, C.; Clifford, S.; Ochterski, J.; Petersson, G. A.; Ayala, P. Y.; Cui, Q.; Morokuma, K.; Malick, D. K.; Rabuck, A. D.; Raghavachari, K.; Foresman, J. B.; Cioslowski, J.; Ortiz, J. V.; Stefanov, B. B.; Liu, G.; Liashenko, A.; Piskorz, P.; Komaromi, I.; Gomperts, R.; Martin, R. L.; Fox, D. J.; Keith, T.; Al-Laham, M. A.; Peng, C. Y.; Nanayakkara, A.; Gonzalez, C.; Challacombe, M.; Gill, P. M. W.; Johnson, B. G.; Chen, W.; Wong, M. W.; Andres, J. L.; Head-Gordon, M.; Replogle, E. S.; Pople, J. A. *Gaussian 98, revision A.6*; Gaussian, Inc.: Pittsburgh, PA, 1998.
(29) Hay, P. J.; Wadt, W. R. *J. Chem. Phys.* **1985**, *82*, 270–283.
(30) Wadt, W. R.; Hay, P. J. *J. Chem. Phys.* **1985**, *82*, 284–298.
(31) Hay, P. J.; Wadt, W. R. *J. Chem. Phys.* **1985**, *82*, 299–310.
(32) Wilson, A. K.; van Mourik, T.; Dunning, T. H. *THEOCHEM* **1996**, *388*, 339–349.
(33) Constantino, E.; Rimola, A.; Rodriguez-Santiago, L.; Sodupe, M. *New J. Chem.* **2005**, *29*, 1585–1593.
(34) Jeanvoine, Y.; Spezia, R. *J. Phys. Chem. A* **2009**, *113*, 7878–7887.
(35) Breneman, C. M.; Wiberg, K. B. *J. Comput. Chem.* **1990**, *11*, 361–373.
(36) Lees, R. M.; Baker, J. G. *J. Chem. Phys.* **1968**, *48*, 5299–5318.
(37) *SAS/STAT User's Guide, Version 6.12*; SAS Institute Inc.: Cary, NC, 2000.
(38) Guàrdia, E.; Sesé, G.; Padró, J. A. *J. Mol. Liq.* **1994**, *62*, 1–16.
(39) Roccatano, D.; Berendsen, H. J. C.; D'Angelo, P. *J. Chem. Phys.* **1996**, *108*, 9487–9497.
(40) Berendsen, H. J. C.; Grigera, J. R.; Straatsma, T. P. *J. Phys. Chem.* **1987**, *91*, 6269–6271.
(41) Berendsen, H. J. C.; Postma, J. P. M.; van Gunsteren, W. F.; Di Nola, A.; Haak, J. R. *J. Chem. Phys.* **1984**, *81*, 3684–3690.
(42) Essmann, U.; Perera, L.; Berkowitz, M. L.; Darden, T.; Lee, H.; Pedersen, L. G. *J. Chem. Phys.* **1995**, *103*, 8577–8593.
(43) Hermes, C.; Gilberg, E.; Koch, M. *Nucl. Instrum. Methods Phys. Res.* **1984**, *222*, 207–214.
(44) Pettifer, R. F.; Hermes, C. *J. Appl. Crystallogr.* **1985**, *18*, 404–412.
(45) Filipponi, A.; Di Cicco, A.; Natoli, C. R. *Phys. Rev. B* **1995**, *52*, 15122–15134.
(46) D'Angelo, P.; Barone, V.; Chillemi, G.; Sanna, N.; Mayer-Klauke, W.; Pavel, N. V. *J. Am. Chem. Soc.* **2002**, *124*, 1958–1967.
(47) D'Angelo, P.; Migliorati, V.; Guidoni, L. *Inorg. Chem.* **2010**, *49*, 4224–4231.
(48) Inada, Y.; Hayashi, H.; Sugimoto, K.-i.; Funahashi, S. *J. Phys. Chem. A* **1999**, *103*, 1401–1406.
(49) Migliorati, V.; Chillemi, G.; Mancini, G.; Zitolo, A.; Tatoli, S.; Filipponi, A.; D'Angelo, P. *J. Phys.: Conf. Ser.* **2009**, *190*, 012057.
(50) Eigen, M. *Pure Appl. Chem.* **1963**, *6*, 97–116.
(51) Chandrasekhar, J.; Jorgensen, W. L. *J. Chem. Phys.* **1982**, *77*, 5080–5089.